Journal of Alloys and Compounds 480 (2009) 970–973

Contents lists available at ScienceDirect

Journal of Alloys and Compounds

journal homepage: www.elsevier.com/locate/jallcom

Synthesis of α-Fe_2O_3 hexagons and their magnetic properties

Chuanhui Xia[a,b], Chenguo Hu[a,*], Yufeng Xiong[c], Na Wang[a]

[a] Department of Applied Physics, Chongqing University, Chongqing 400044, PR China
[b] Science College of Chongqing Jiaotong University, Chongqing 400074, PR China
[c] National Center for Nanoscience and Technology, Beijing, 100080, PR China

ARTICLE INFO

Article history:
Received 20 August 2008
Received in revised form 23 February 2009
Accepted 24 February 2009
Available online 9 March 2009

Keywords:
Oxide materials
Solid state reactions
Magnetization
Magnetic measurement

ABSTRACT

α-Fe_2O_3 hexagons are synthesized by a composite-hydroxide-mediated (CHM) method at temperature of 200 °C for 24 h. The X-ray diffraction of the synthesized α-Fe_2O_3 sample demonstrates a hexagonal phase with space group of $R\bar{3}c$(167) and lattice constants of a = 5.00 Å and c = 13.62 Å. Scanning electron microscopy shows well dispersed hexagons with an average diameter of 3 μm and a thickness of 300–500 nm. The magnetic properties of the hexagons were also investigated. The plot of magnetization versus temperature (M–T) from 100 to 300 K under an applied field of 1000 Oe indicates that the Morin transition temperature is about 220 K, lower than the normal value (263 K) of bulk α-Fe_2O_3. The hysteresis loop exhibits weak ferromagnetic properties at temperature of 300 K. The curve of magnetization versus an applied magnetic field (M–H) at temperature of 10 K reveals the antiferromagnetic and hysteretic behaviors caused by surface spin disorder.

1. Introduction

Iron oxide and oxyhydroxide iron have been extensively used in the production of pigments, catalysts, gas sensors, magnetic recordings, and raw materials for hard and soft magnets [1–7]. Among the iron oxides, α-Fe_2O_3 has the corundum structure, while γ-Fe_2O_3 and Fe_3O_4 have the spinel structure. γ-Fe_2O_3 and Fe_3O_4 are metastable in the oxidative atmosphere and can be oxidized to α-Fe_2O_3 by being heated to over 400 °C [8]. The magnetic properties of α-Fe_2O_3 have been studied extensively both in bulk and nanoparticle form. Bulk α-Fe_2O_3 has a first-order magnetic transition at T_M = 263 K, which is called the Morin transition. Below 263 K, the spin is oriented in antiparallel directions along c-axis, and the material behaves like a uniaxial antiferromagnet. Between 263 and 960 K (Néel temperature), the spin shows slight canting and weak ferromagnetism [9].

It has been observed that crystals with different morphology and size possess dissimilar magnetic properties [10–18]. Recently, Zeng et al. [15] prepared α-Fe_2O_3 nanorods with a diameter of about 30 nm and length up to 500 nm. The magnetic measurement of the nanorods exhibited a weak ferromagnetism with the coercive force of 584 Oe and the remanence of 0.039 emu/g at a temperature of 5 K, indicating that the coercivity depends on aspect ratio. But, Zeng et al. failed to observe the Morin transition of the α-Fe_2O_3 nanorods. Wang et al. [10] synthesized spherical α-Fe_2O_3 nanoparticles with a diameter of about 50 nm which display weak ferromagnetic behavior with a remnant magnetization (Mr) of 0.065 emu/g and a coercivity of 219 Oe. Tadić et al. [14] prepared α-Fe_2O_3/SiO_2 nanocomposites containing 30 wt% of α-Fe_2O_3. Magnetic measurements found the sample did not exhibit the Morin transition down to 2 K. In this paper, we present the synthesis of the α-Fe_2O_3 hexagons for the first time by CHM approach. The method is based on the reactions of source materials in eutectic

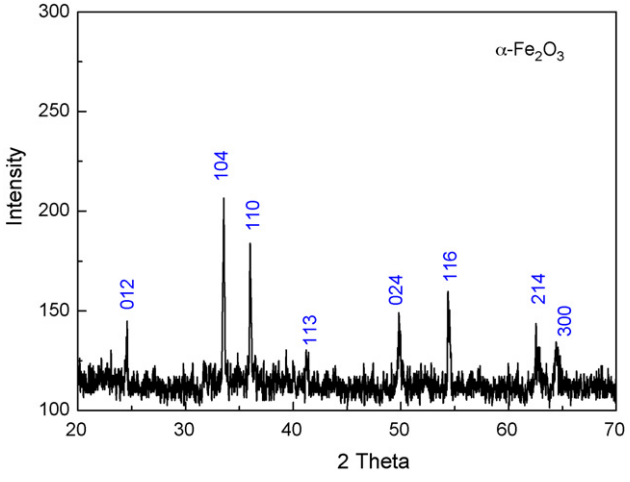

Fig. 1. XRD spectrum of the synthesized α-Fe_2O_3.

* Corresponding author. Tel.: +86 23 65104741; fax: +86 23 65111245.
E-mail address: hucg@cqu.edu.cn (C.H. Hu).

0925-8388/$ – see front matter © 2009 Elsevier B.V. All rights reserved.
doi:10.1016/j.jallcom.2009.02.106

composite-hydroxide melts at temperature of ~200 °C and at atmospheric pressure without using organic dispersant or capping agent [19–23]. The as-synthesized α-Fe_2O_3 hexagons were characterized by X-ray diffraction (XRD), scanning electron microscopy (SEM) and transmission electron microscopy (TEM). The magnetic properties of the α-Fe_2O_3 hexagons were also investigated.

2. Experimental

Single crystalline α-Fe_2O_3 hexagons were prepared by the CHM method from $FeCl_3$. All reactants were of analytical grade. In a typical experiment, 9 g mixed NaOH and KOH with Na/K ratio of 51.5:48.5 was first placed in a 25 mL Teflon vessel and then 1 mmol of $FeCl_3$ was added. Second, the vessel was placed in a furnace preheated to 200 °C for 30 min to insure that the hydroxides were totally molten, then the vessel was taken out and shaken in order to mix reactants completely. Third, the Teflon vessel was put back into the furnace and incubated for 24 h. The vessel was taken out and allowed to cool to room temperature. Finally, the obtained product was washed with deionized water several times to remove excess hydroxide on the surface of the particles.

XRD, SEM (field emission Hitachi-S4800) and TEM were used to characterize the crystalline phase, the morphology, the size and the structure of the synthesized α-Fe_2O_3 hexagons. Magnetic measurements were obtained using Quantum's PPMS-9 vibrating sample magnetometer. *M–T* curves were measured under a field cooled mode at an applied magnetic field of 1 kOe and in the field range of $-15\ \text{kOe} < H < 15\ \text{kOe}$ at temperatures of 10 and 300 K.

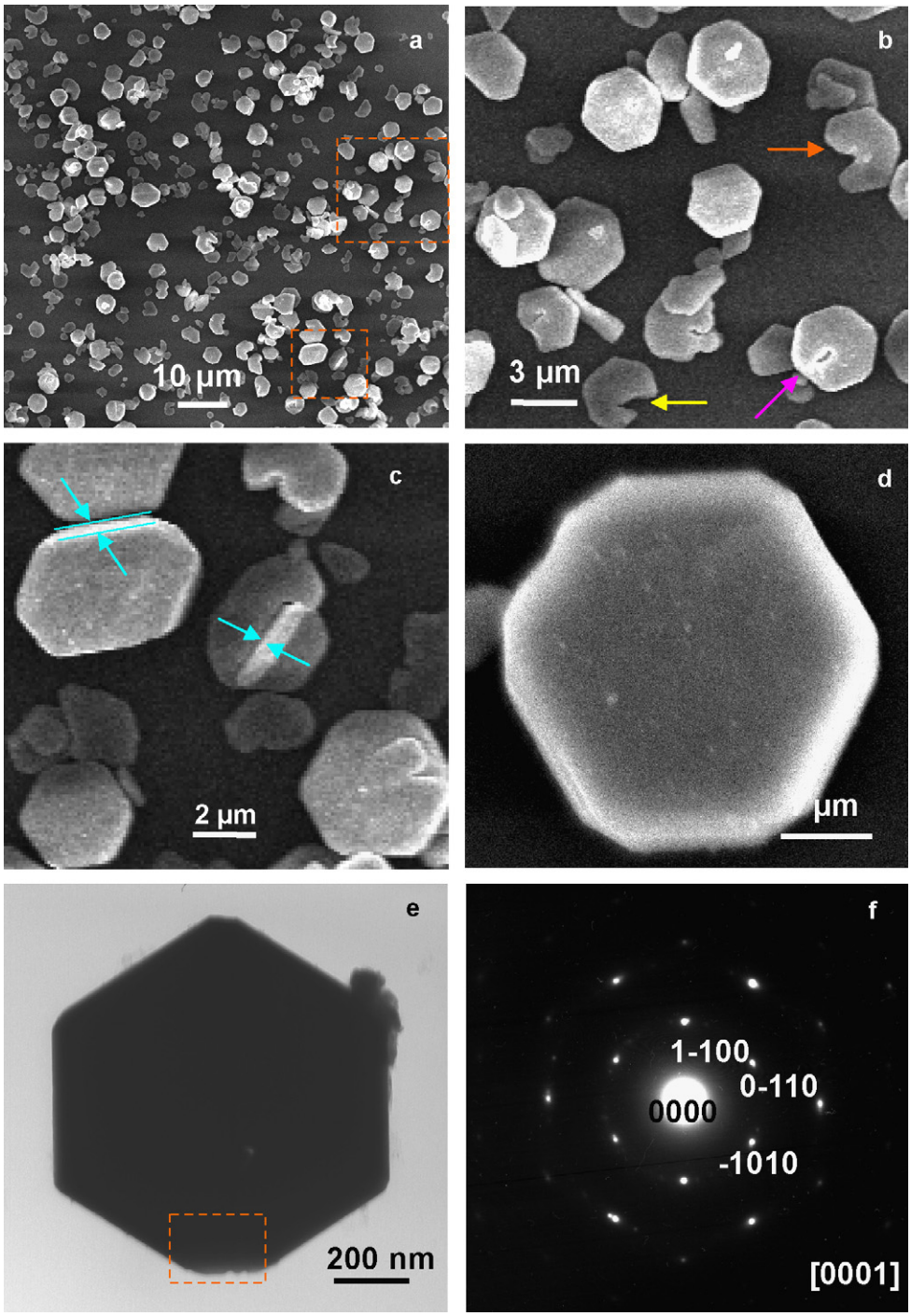

Fig. 2. SEM images of the synthesized α-Fe_2O_3, (a) low magnified images, (b–d) high magnified images, (e) TEM image and (f) electron diffraction pattern of the synthesized α-Fe_2O_3.

3. Results and discussion

Fig. 1 shows the XRD spectrum of the synthesized α-Fe_2O_3 hexagons. All the peaks can be indexed to hexagonal phase [space group: $R\bar{3}c(167)$] of α-Fe_2O_3 (JCPDS No.840311) with lattice constants of $a = 5.00$ Å and $c = 13.62$ Å. No peak from impurities was found in the XRD spectrum. The diffraction peaks suggest that the powder is well crystallized. Fig. 2a reveals that the synthesized α-Fe_2O_3 is dispersed particles. Fig. 2b and c are magnified images of the selected areas in Fig. 2a. From these images, we can see that these particles are hexagons with an average diameter of 3 μm and thickness of 300–500 nm. However, there are some irregular or defective hexagons, as pointed out by the arrows in Fig. 2b. Fig. 2d shows the SEM image of a magnified individual hexagonal crystal. Fig. 2e and f exhibit the TEM image and electron diffraction pattern of the hexagonal crystal. The electron diffraction pattern of the selected area marked in Fig. 2e indicates that the hexagon is a single-crystal and hexagon plane is (0 0 0 1) plane.The formation of Fe_2O_3 resulting from the chemical reactions in the hydroxide melts is shown below:

$$FeCl_3 + 3NaOH \rightarrow Fe(OH)_3 + 3NaCl$$

With the continuous heating, $Fe(OH)_3$ decomposes to form Fe_2O_3 gradually.

$$Fe(OH)_3 \rightarrow Fe_2O_3 + H_2O$$

KOH reacts with $FeCl_3$ in the same way NaOH does. Here we only include NaOH in the formula for simplicity. NaOH and KOH play the role of reaction medium in the process of crystal growth, but they can be removed completely by washing with deionized water and do not appear in the final target product.

It is well known that morphology, particle size, and synthetic route would affect properties of a material. We have mentioned that there are many reports about the magnetism of α-Fe_2O_3 particles in shapes of sphere, rod, nanowire and shuttle [15,16,10]. However, there has not been any report about α-Fe_2O_3 in hexagon shape. Therefore, the study of the magnetic property of the α-Fe_2O_3 hexagons is a novel work. It is widely accepted that Morin transition can be explained by the competition of two kinds of anisotropies [24]: the single ion anisotropy K_{fs} caused by the spin-orbit coupling tends to make the spin align along(1 1 1) axis, and the magnetic dipole anisotropy K_{md} makes the spin align in (1 1 1) plane. Thus, the Morin transition temperature has been found to be strongly dependent on the particle size, decreasing with the reduction of particle size or even vanishing with a diameter less than 8 nm for spherical particles [25,26]. Strains and crystal defects, such as low crystallinity, vacancies, stoichiometric deviation and surface effects also tend to reduce T_M [27].

Fig. 3 shows the curve of the temperature-dependent magnetization from 100 to 300 K under an applied field of 1000 Oe. The temperature at which $M = M_S/2$ corresponds to T_M [28]. The value of T_M is 220 K, lower than the normal value (263 K) of bulk α-Fe_2O_3 [15]. This fits the expected trend of decreasing T_M as the particle size decreases. The majority of α-Fe_2O_3 hexagons have an average diameter of 3 μm and thickness of 300–500 nm. As there are still some small particles in the products with thickness less than 100 nm, the

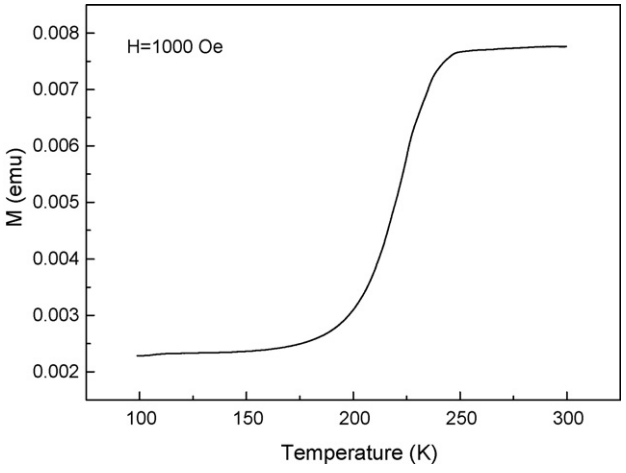

Fig. 3. M–T plot of the synthesized α-Fe_2O_3 under the applied magnetic field of 1000 Oe.

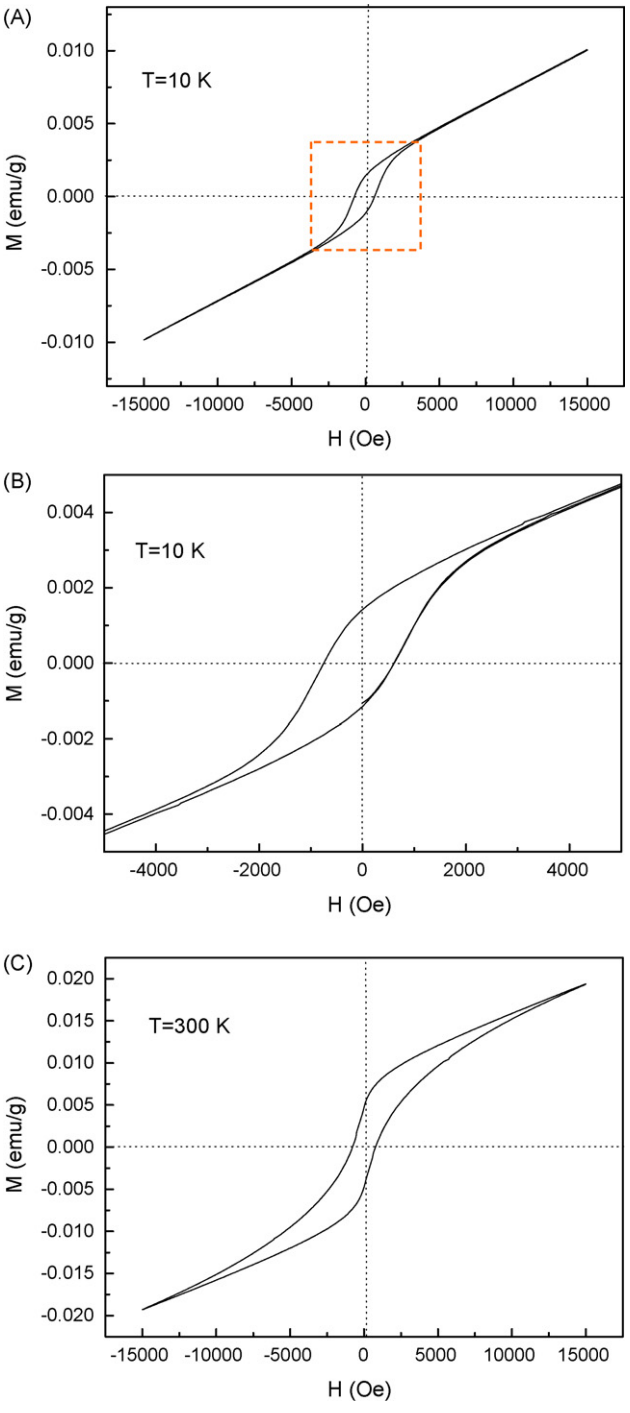

Fig. 4. Hysteresis loop for the synthesized α-Fe_2O_3 at temperature of 10 K (a–b) and 300 K (c).

decrease in the size of the particles is most likely the reason for the decrease in T_M.

Fig. 4a–c shows the M–H curves of the α-Fe_2O_3 hexagons at 10 and 300 K respectively. From Fig. 4a, we can see that the magnetization increases almost linearly under an applied magnetic field up to 5000 Oe. Saturated magnetization was not observed even under an applied magnetic field up to 15000 Oe. The linear increase in the $M(H)$ represents the contribution of the α-Fe_2O_3 hexagon antiferromagnetic core [14], which is consistent with the feature of lower T_M. When the spin is oriented in antiparallel directions along c-axis, the material behaves like a uniaxial antiferromagnet. Fig. 4b shows the hysteresis loop between 0 and 5000 Oe, with the remanence magnetization (M_r) of 1.48×10^{-3} emu/g and coercivity (H_c) of 700 Oe. Hysteretic behavior is the result of surface spin disorder [14]. The observed coercivity of the α-Fe_2O_3 hexagons is larger than that of the rod, sphere and shuttle-like α-Fe_2O_3 [15,16,10] further indicating that the magnetization of ferromagnetic materials is sensitive to microstructural characteristics such as size, shape and defects in crystal structure. [10,17,29]. Fig. 4c shows the magnetic hysteresis loop at 300 K. We failed to observe saturation of the magnetization even under the maximum applied magnetic field. The α-Fe_2O_3 hexagons display weak ferromagnetic behavior with the remanence magnetization (M_r) of 4.9×10^{-3} emu/g and coercivity (H_c) of 1.25 kOe.

4. Conclusion

Well dispersed α-Fe_2O_3 hexagons have been synthesized for the first time by using a composite-hydroxide-mediated (CHM) method. The average diameter is 3 μm and the thickness is 300–500 nm. The M–T plot shows the Morin transition temperature is about 220 K, lower than the normal value (263 K) of bulk α-Fe_2O_3 due to the decreasing T_M as the particle size decreases. The linear change of M–H curves at temperature of 10 K represents the contribution of the hexagon antiferromagnetic core. The hysteresis loop obtained from the change of the magnetic field between 0 and 5000 Oe is attributed to the surface spin disorder. The hysteresis loop at 300 K displays weak ferromagnetic behavior with a lack of magnetic saturation owing to shape anisotropy.

Acknowledgments

This work has been funded by the NSFC (20741006). The authors thank Mr. Bryan Baker in MSE at Georgia Tech for English language editing.

References

[1] C. Gong, D. Chen, X. Jiao, Q. Wang, J. Mater. Chem. 12 (2002) 1844–1847.
[2] E. Matijevic, P. Scheiner, J. Colloid Interf. Sci. 63 (1978) 509–524.
[3] M.P. Morales, T.G. Carreño, C.J. Serna, J. Mater. Res. 7 (1992) 2538–2545.
[4] B. Faust, M. Hoffmann, D. Bachnemann, J. Phys. Chem. 93 (1989) 6371–6381.
[5] J. Kiwiand, M. Cratzel, Faraday Trans. 83 (1987) 1101–1108.
[6] T. Teranishi, A. Wachi, M. Kanehara, T. Shoji, N. Sakuma, M. Nakaya, J. Am. Chem. Soc. 130 (2008) 4210–4211.
[7] K. Siroky, J. Jiresová, L.O. Hudec, Thin Solid Films 245 (1994) 211–214.
[8] Z.Y. Ma, F.S. Li, P. Cui, H.P. Bai, Chin. J. Catal. 24 (2003) 795–798.
[9] J.S. Jiang, L. Gao, X.L. Yang, J.K. Guo, Acta Phys.-Chim. Sin. 16 (2000) 312–316.
[10] S.F. Wang, H.M. Cao, F. Gu, C.Z. Li, G.J. Huang, J. Alloys. Compd. 457 (2008) 560–564.
[11] X.J. Zhang, Q.L. Li, Mater. Lett. 62 (2008) 988–990.
[12] Q. Han, Z.H. Liu, Y.Y. Xu, H. Zhang, J. Cryst. Growth 307 (2007) 483–489.
[13] Z.G. Li, W.P. Cai, G.T. Duan, P.S. Liu, Physica E 40 (2008) 680–683.
[14] M. Tadić, D. Marković, V. Spasojević, V. Kusigerski, M. Remškar, J. Pirnat, Z. Jagličić, J. Alloys. Compd. 441 (2007) 291–296.
[15] S.Y. Zeng, K.B. Tang, T.W. Li, J. Colloid Interf. Sci. 312 (2007) 513–521.
[16] X.M. Liu, S.Y. Fu, H.M. Xiao, C.J. Huang, J. Solid State Chem. 178 (2005) 2798–2830.
[17] X.H. Liu, G.Z. Qin, A.G. Yan, Z. Wang, X.G. Li, J. Alloys. Compd. 433 (2007) 216–220.
[18] Y.C. Zhang, J.Y. Tang, X.Y. Hu, J. Alloys. Compd. 462 (2008) 24–28.
[19] C.G. Hu, H. Liu, C.S. Lao, L.Y. Zhang, D. Davidovic, Z.L. Wang, J. Phys. Chem. B 110 (2006) 14050–14054.
[20] C.G. Hu, Z.W. Zhang, H. Liu, P.X. Gao, Z.L. Wang, Nanotechnology 17 (2006) 1987–5983.
[21] C.G. Hu, H. Liu, W.T. Dong, Y.Y. Zhang, G. Bao, C.S. Lao, Z.L. Wang, Adv. Mater. 19 (2007) 470–474.
[22] N. Wang, C.G. Hu, C.H. Xia, B. Feng, Z.W. Zhang, Y. Xi, Y.F. Xiong, Appl. Phys. Lett. 90 (2007) 163111.
[23] Z.W. Zhang, C.G. Hu, Y.F. Xiong, R.S. Yang, Z.L. Wang, Nanotechnology 18 (2007) 465504.
[24] A. Tasali, S. Iida, J. Phys. Soc. Jpn. 16 (1961) 1697.
[25] N. Amin, S. Arajs, Phys. Rev. B 35 (1987) 4810–4811.
[26] R.D. Zysler, M.V. Mansilla, D. Fiorani, Eur. Phys. J. B 41 (2004) 171–175.
[27] M.Z. Dang, D.G. Rancourt, J.E. Dutrizac, G. Lamarche, R. Provencher, Hyperfine Interact. 117 (1998) 271–319.
[28] G.H. Wang, X.P. Zhong, Q. Wang, H.L. Luo, D.L. Hou, J. Appl. Phys. 70 (1991) 5906–5908.
[29] M. Sorescu, R.A. Brand, D.M. Taravasanu, L. Diamandescu, J. Appl. Phys. 85 (1999) 5546–5548.